DOI: 10.1002/chem.200700125

Discotic Liquid-Crystalline Materials Based on Porphycenes: A Mesogenic Metalloporphycene–Tetracyanoquinodimethane (TCNQ) Adduct

Marcin Stępień,[a, c] Bertrand Donnio,[b] and Jonathan L. Sessler*[a]

Abstract: A number of substituted zinc(II) porphycenes and porphyrins have been synthesized as potentially mesogenic materials. One of the resulting porphycenes, bearing eight decyloxy chains, exhibits two mesophases, a transient lamellar phase (Lam) and a highly ordered lamello-columnar phase (L_{Col}), with remarkably different structural characteristics. The same zinc(II) porphycene also forms an electron donor–acceptor (EDA) complex with tetracyanoquinodimethane (TCNQ), generating a hexagonal columnar mesophase (Col_h) that is thermally stable up to ca. 200 °C. The EDA interaction between porphycene and TCNQ has been probed using electronic and vibrational spectroscopy. A mixture of zinc(II) porphyrins, isomeric with the above porphycene complex, forms a rectangular columnar mesophase (Col_r).

Keywords: donor–acceptor systems · liquid crystals · metallomesogens · porphyrinoids · X-ray diffraction

Introduction

Since the report of the first discotic mesogens by Chandrasekhar in 1977,[1] this class of liquid crystals has attracted considerable attention.[2–4] Discotic mesogens are of interest because their unusual structural features often result in unique physical properties that may be employed in the construction of functional organic materials.[5] In particular, discotic mesogens have shown promise as organic conductors with enhanced carrier mobilities,[6,7] high-efficiency photodiodes,[8–11] and optoelectronic data storage media.[12] Most discotic mesogens are built around large π-electron systems, both carbo- and heterocyclic, such as triphenylenes,[13] coronenes,[14] phthalocyanines, or porphyrins.[15] The properties of the aromatic core affect not only the stability of the mesophase but also its electronic and optical characteristics.[16]

The porphyrin ring is an extremely valuable structural motif for the construction of mesogens and metallomesogens.[17] It can coordinate a wide range of metal ions and is available with a range of peripheral substitution, some of which are fairly easy to synthesize. These features not only provide for structural diversity but also allow the electronic and optical properties to be fine-tuned. To date, discotic mesogens have been obtained from both *meso*- and β-substituted porphyrins bearing a variety of functional groups.[10,18–30] Generally, all the substituents are identical, but unsymmetrically substituted porphyrin discotics are also known.[29] In most cases, zinc coordination confers the greatest stability on the porphyrin-based mesophases; however, other ions, such as Cu^{II},[27] Mo^{V},[23] Si^{IV},[30] and V^{IV},[26] have been studied and have also proved effective.[17]

A potentially interesting class of mesogens can be obtained by appropriate functionalization of porphyrin analogues (porphyrinoids). This family of macrocycles, characterized by unusual structural diversity, includes expanded,[31,32] contracted,[33] and isomeric[34] porphyrins, as well as a range of core-modified systems.[35,36] Consequently, porphyrin analogues possess many intriguing properties, such as extremely strong and red-shifted electronic absorptions,[37] controllable conformational flexibility,[38] or the ability to bind anions,[34,39] features that might lead to liquid-crystal systems with unusual functionalities. Unfortunately, the task of making a mesogenic porphyrinoid combines the usual

[a] Dr. M. Stępień, Prof. J. L. Sessler
Department of Chemistry & Biochemistry
University of Texas, 1 University Station A5300
Austin, TX 78712 (USA)
Fax: (+1) 512-471-7550
E-mail: sessler@mail.utexas.edu

[b] Dr. B. Donnio
Institut de Physique et Chimie des Matériaux de Strasbourg
UMR 7504 (CNRS-Université Louis Pasteur), 23 rue du Loess BP 43
67034 Strasbourg Cedex 2 (France)

[c] Dr. M. Stępień
Present address: Wydział Chemii, Uniwersytet Wrocławski
ul. F. Joliot-Curie 14, 50-383 Wrocław (Poland)

Supporting information for this article is available on the WWW under http://www.chemeurj.org/ or from the author.

challenges of liquid-crystal research (design difficulties, tedious preparation of homologues, purification problems) with those of porphyrinoid chemistry (low yields, instability of intermediates, etc.). Recently we reported the first discotic liquid crystals based on expanded porphyrins.[40–42] The first of these, a system called hydrazinophyrin, was characterized as a free base and was found to exist as a columnar mesophase as judged from polarizing optical microscopy.[40] A second liquid crystalline system was obtained by preparing the uranyl complexes of a hexaazamacrocycle called alaskaphyrin.[42] Both of these mesogens were Schiff-base derived and hence inherently susceptible to hydrolytic instability. Recently, however, we found that mesomorphic behavior could also be induced in appropriately substituted cyclo[8]pyrroles by addition of electron-acceptor molecules, such as polynitroaromatics.[41] These supramolecular liquid crystals are of interest because of the unique optical properties of cyclo[8]pyrrole and because of their potential utility as explosives sensors.

In the present contribution we describe our efforts to prepare metallomesogens based on porphycene, an artificial macrocyclic system isomeric with porphyrin. Porphycene, also known as [18]porphyrin(2.0.2.0), originally synthesized in 1986 by Vogel and co-workers,[43] was the first porphyrin isomer to be reported in the literature. Subsequent studies showed that its chemistry and physical properties often depart in significant ways from those of the parent porphyrin macrocycle.[31] One of the key differences involves the optical signature (porphycenes are blue rather than purple). This, in turn, has led us to consider that porphycene-based discotic mesphases could be of interest as potential photodiode materials since, at least in principle, they might be expected to respond to different wavelengths than systems based on porphyrins. Therefore, we decided to check whether the porphycene ring meets the structural requirements necessary for mesophase formation. Toward this end, we synthesized two functionalized porphycenes **1a**,**b** (Scheme 1) and explored their phase behavior. Additionally, two complementary porphyrin systems **2a**,**b** were obtained as isomeric mixtures and studied in parallel with porphycenes **1a**,**b**. We found that both the porphycene and porphyrin derivatives bearing a greater number of alkoxy chains (**1b** and **2b**) gave rise to liquid crystalline behavior, but that the nature of the mesogens formed from the two cores differed. We also found that the addition of the electron deficient agent tetracyanoquinodimethane (TCNQ) to the porphycenes helped stabilize the formation of liquid crystalline phases.

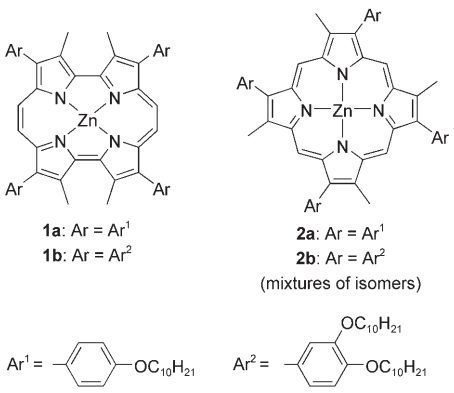

Scheme 1.

Results and Discussion

Synthesis of porphycenes and porphyrins: As in the case of porphyrins and the other porphyrinoid systems alluded to above, we felt the most straightforward approach to producing mesogenic materials or those in which liquid crystallinity could be induced by addition of an appropriate additive (so-called protomesogens) would involve peripheral substitution with appropriately chosen solubilizing "tails". However, unlike porphyrins, in porphycenes the *meso* positions are not uniformly distributed around the ring. Therefore, we considered that *meso*-functionalization would be less likely to provide discotic mesophases and, accordingly, decided to focus on the construction of β-substituted porphycenes. As a general rule, β-substituted porphycenes are also better ligands for metal cations than the corresponding *meso* derivatives, a feature that was expected to abet metal insertion once the putative mesogens were constructed. With these considerations in mind, and taking into account some of the successful substitution patterns known to induce mesomorphism in regular porphyrins,[21,27] structures **1a**,**b** were chosen as specific targets.

The requisite β-substituted pyrroles **4a**,**b** were obtained in two steps using the method of Zard and Barton (Scheme 2).[44] Further steps followed the established route to β-octasubstituted porphycenes,[45] and started with iodination of **4** to the iodopyrrole **5**, which was then converted into the respective bipyrrole **6** using Ullman coupling. Diester **6** was then saponified and decarboxylated to yield the α-free bipyrrole **7**, which was subsequently formylated (to give **8**) under Vilsmeier conditions. Free base porphycenes **9a**,**b** were then obtained by subjecting precursors **8a**,**b** to McMurry coupling. Subsequent metal insertion provided the desired zinc complexes **1a**,**b**.

Reduction of pyrroles **4a**,**b** afforded the unstable carbinols **10a**,**b**, which were subjected to silica-catalyzed self-condensation,[46] followed by oxidation with DDQ. In analogy to what has been observed in the case of other acid-catalyzed condensations involving activated pyrroles, this reaction proceeds reversibly in the case of **10a**,**b**, and necessarily results in "scrambling" of the substitution pattern.[46,47] As a consequence, the free-base porphyrins **11a**,**b** were obtained as inseparable mixtures of isomers **I**–**IV** (Scheme 3). These mixtures were then converted into the corresponding zinc complexes **2a**,**b**, which likewise could not be separated into the individual components.

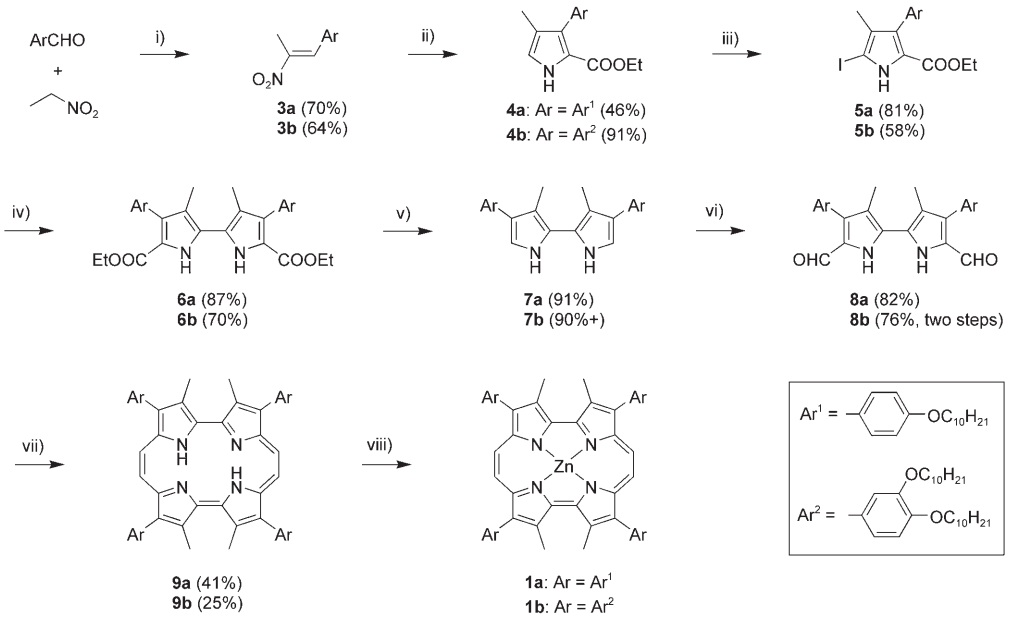

Scheme 2. Synthesis of Zn porphycenes **1a**,**b**: i) $AcONH_4$; ii) $CNCH_2COOEt$, THF/*i*PrOH, DBU; iii) I_2, NaI, $NaHCO_3$, DCE, H_2O, Δ; iv) 1) Boc_2O, DMAP, CH_2Cl_2, 2) Cu, toluene, Δ, 3) 180 °C, vacuum; v) KOH, glycol, 200 °C; vi) 1) $POCl_3$, DMF/DCE, Δ, 2) AcONa, H_2O, Δ; vii) $TiCl_4$, Zn, CuCl, THF, Δ; viii) $Zn(OAc)_2$, $CHCl_3$, MeOH, Δ.

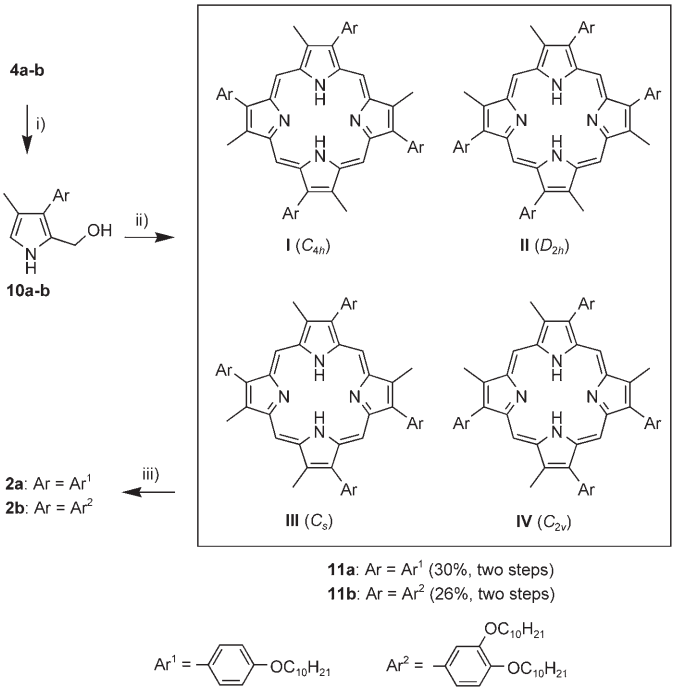

Scheme 3. Synthesis of Zn porphyrins **2a**,**b**: i) $LiAlH_4$, THF; ii) 1) silica gel, CH_2Cl_2, 2) DDQ; iii) $Zn(OAc)_2$, $CHCl_3$, MeOH, Δ.

Phase behavior of porphycene complexes: The transitional properties of compounds **1a**,**b** were investigated using polarizing optical microscopy (POM), differential scanning calorimetry (DSC) and X-ray diffraction (XRD). The resulting temperature data, mainly corresponding to DSC measurements, are summarized in Table 1. Compound **1a** exhibits

Table 1. Thermodynamic data for the zinc complexes of porphycenes and porphyrins.

Compound	Transitional properties[a]				
1a	Cr_1	207 [34]	Cr_2	223 [39]	I
1b	{Lam}	55[b]	L_{Col}	≈90 [≈17]	I
1a·DMAP			Cr	255 [41]	I
1b·DMAP			Cr	123 [43]	I
1b·*n*TCNQ	Cr	≈110[b]	Col_h	170–200[c]	I
2a			Cr	146 [35]	I
2b			Col_r *c*2*mm*	90 [17]	I

[a] Transition temperatures are given in °C, and the corresponding enthalpy changes are included in square brackets [ΔH in kJ mol^{-1}]. Cr, Cr_1, Cr_2 refer to phases that are crystalline or solid; Col_r and Col_h to rectangular and hexagonal columnar phase, respectively; Lam, lamellar phase; L_{Col}, lamello-columnar phase; I, isotropic liquid. [b] Determined from variable-temperature XRD analyses. [c] Range of clearing points observed for different batches by POM and XRD.

two phase transitions, at 207 and 223 °C, both of which show good reversibility and display enthalpies exceeding 30 kJ mol^{-1}. The high enthalpy value observed for the second transition provides support for the postulate that the intermediate phase is not a liquid crystal. Indeed, the phase showed low fluidity and its XRD pattern was typical of a crystalline material (cf. Supporting Information). It was therefore concluded that **1a** exhibits temperature-dependent polymorphism and both of its anisotropic phases are crystalline.

The phase behavior of compound **1b** is more complicated and was partly elucidated using X-ray diffraction (XRD) analysis. In its initial form, obtained by evaporation from a dichloromethane solution, **1b** exists as a metastable lamellar mesophase (Lam) from room temperature up to about 55 °C. On further heating, the Lam phase transforms into a

more ordered phase, which was identified as lamello-columnar (L_{Col}) on the basis of XRD, before finally clearing to produce an isotropic liquid at 90 °C. When this latter isotropic species is allowed to cool slowly, only the L_{Col} phase is produced as inferred from XRD analysis. Several DSC cycles were performed for **1b** at different scan rates and with different intervals between scans. On the basis of these analyses, it is proposed that the Lam phase (and possibly another unidentified phase) may be recovered from the isotropic liquid phase under certain conditions. Unfortunately, this interpretation is tentative since the isotropic liquid of **1b** is prone to supercooling and the DSC results are not fully conclusive.

The XRD pattern of the **1b** Lam phase recorded at 50 °C is shown in Figure 1. Two sharp reflections in the small-angle part at 30.5 and 15.15 Å with a 1:2 ratio were observed and considered indicative of a lamellar structure. Two additional broad scattering halos were also seen at 4.4 Å (ascribed to the molten chains) and at 8.8 Å (reflecting double periodicity) that are indicative of a liquid-like phase. For a smectic phase derived from **1b**, a mapped out chain area, A_{ch}, of about 28 Å^2 can be deduced (assuming four chains on each end of the molecule), in reasonable agreement with the value expected for the cross-sectional area of a molten aliphatic chain in a smectic phase.

The absence of features ascribable to offset or face-to-face stacking interactions, which is remarkable for such planar molecules, has previously been noticed in the discotic lamellar phases reported by Ohta et al. for certain related

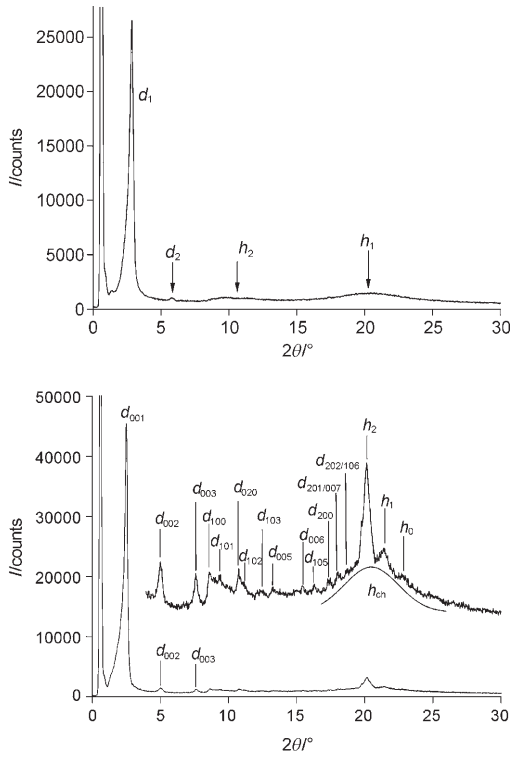

Figure 1. X-ray diffraction pattern obtained for **1b** at 50 °C (top) and 80 °C (bottom).

mesogenic *meso*-tetraarylporphyrins.[27] In the present case, this smectic-like arrangement can be explained by considering the conformational flexibility of **1b**. Each molecule of **1b** adopts a conformation that is not discoid but lath-like, with the lateral chains stretching in opposite directions (see also the later discussion of the L_{Col} phase). Furthermore, the absence of apparent π–π interactions is consistent with there being little if any translational order within the layer. As the rotation of the laths within the layer is hindered, the phase may be referred to as a "biaxial" smectic-like phase. Phases of this kind (discotic lamellar) have been documented for other discotic systems.[48]

The XRD pattern recorded for **1b** at 80 °C (Figure 1) is indicative of the formation of a lamello-columnar mesophase (L_{Col}), similar to those observed recently for lath-like perylene diimides[49] and for disc-lath mixtures of phthalocyanines and perylenes.[50] Three sharp reflections, with reciprocal spacings in the ratio 1:2:3, are observed in the small-angle region at 34.8, 17.5, and 11.55 Å, respectively. Accordingly, these are assigned as (001), (002), and (003) reflections. The presence of these higher order features indicates that the layered structure is very pronounced. Two broad halos were observed in the wide-angle part, corresponding to the liquid-like order of the molten chains (h_{ch} at 4.5 Å) and to the stacking of the flat molecular cores (h_0 at 3.5 Å). Additionally, two sharp wide-angle peaks are seen at 4.15 and 4.4 Å that are ascribed to specific interactions between aromatic cores. These assigned interactions likely correspond to an intermolecular in-plane ordering, such as columnar stacking within the layers (ribbons of columns). Finally, a number of less intense, but nevertheless sharp reflections appear in the middle-angle range that could be successfully indexed as ($h0l$) with $h=1$ and 2 and $l=0$, 1, 2, 3, and 5 in a monoclinic system. The resulting indexation provides a very good agreement between the experimental and calculated reciprocal spacings (Table 2). An additional reflection at 8.3 Å was indexed as (020) for reasons given below. The resulting elementary monoclinic cell has a volume of ca. 6000 Å^3, corresponding to approximately two molecules of **1b**.

Based on the comparison of the cell dimensions derived from XRD with the molecular dimensions of **1b** obtained from molecular modeling, a structural model of the L_{Col} phase is proposed (Figure 2). As a consequence of the geometry of the porphycene ring and the substitution pattern employed, it is proposed that molecules of **1b** assume a lath-like conformation with the alkyl chains aligned parallel to the long axis of the lath, as in the Lam phase described above. With the chains fully outstretched, the longer dimension of **1b** becomes ca. 40 Å, comparable to the c lattice constant of the L_{Col} phase ($c=35.4$ Å, the chains being partly molten, and the cores tilted). The L_{Col} phase can therefore be imagined to form smectic layers parallel to the ab plane. The next step was to determine how these layers were packed. This was done as outlined below.

To determine the packing arrangement in **1b** at 80 °C, the value of the cell constant b was determined based on a

Table 2. XRD data for liquid crystalline phases derived from compounds **1** and **2**.

Phase and parameters[d,e]	d_{exp}/Å[a]	00*l*/*hkl*/*hk*[b]	I[c]	d_{theo}/Å[a,d]
1b, Lam, 50 °C	30.5	001	VS	30.4
d = 30.5 Å	15.15	002	M	15.2
V_{mol} = 3350 Å^3	8.8	*h*	br	
A_{mol} = 110 Å^2	4.4	h_{ch}	br	
A_{ch} = 27.5 Å^2				
1b, L_{Col}, 80 °C	34.8	001	VS	34.8
a = 10.42 Å	17.4	002	M	17.4
b = 16.6 Å	11.55	003	M	11.6
c = 35.4 Å	10.25	100	M	10.25
β = 100.54°	9.4	101	M	9.4
V_{cell} = 6020 Å^3	8.3	020	M	8.3
V_{mol} = 3400 Å^3	8.2	102	W	8.2
$Z \approx 2$	7.15	103	W	7.07
	6.95	005	VW	6.96
	5.9	006	VW	5.8
	5.4	105	W	5.3
	5.1	200	W	5.1
	4.95	201/007	W	4.95/4.97
	4.7	202/106	W	4.7
	4.5	h_{ch}	VS	
	4.4	h_2	S	
	4.15	h_1	W	
	3.95	h_0		
2b, Col_r *c2mm*, 70 °C	29.7	20	VS	29.7
a = 59.4 Å	26.35	11	VS	26.35
b = 29.4 Å	16.25	31	M	16.4
S = 1745 Å^2	13.15	22	W	13.15
S_{col} = 872.5 Å^2	10.9	51	VW	11.0
V_{mol} = 3350 Å^3	10.4	42	W	10.45
N_{col} = 1	8.8	33	VW	8.8
$h = V_{mol}/S_{col}$ = 3.83 Å	8.1	71	W	8.15
	7.55	53	VW	7.55
	4.6	h_{ch}	broad	
	3.8	h_0	sharp	
1b·*n*TCNQ, Col_h, 140 °C	24.94	10	VS	25.01
a = 28.9 Å	14.5	11	S	14.45
S = 722.25 Å^2	12.5	20	S	12.5
V_{mol} = 3945 Å^3 (1:1)	8.15	*h*	broad	
d = 5.46 Å (1:1)	4.6	h_{ch}	broad	
V_{mol} = 7525 Å^3 (2:1)	3.3	h_0	sharp	
d = 10.42 Å (2:1)				

[*a*] d_{exp} and d_{theo} are the experimentally measured and theoretical diffraction spacings, respectively. The distances are given in Å. [b] 00*l*/*hkl*/*hk* are the Miller indices of the reflections of 1D lamellar, 3D L_{Col}, and 2D Col phases, respectively. [c] Intensity of the reflections: VS very strong, S strong, M medium, W weak, VW very weak. Derivation of lattice parameters is given in the Experimental Section.

single reflection at 8.3 Å. At first, this reflection was assumed to be (010). With this assumption, the calculated cell volume (≈3000 Å^3) corresponds to approximately one molecule of **1b**. However, the width of the porphycene core, estimated as 13.7 Å, exceeds both the *a* constant and the proposed value of *b*. Based on this mismatch, it was concluded that the reflection at 8.3 Å is in fact (020) and the actual (010) peak is not observed. The molecules can then be fitted onto the *ab* plane according to the "herringbone" packing pattern typical of aromatic molecules,[51] an alignment that was actually observed in the crystal structure of Vogel's

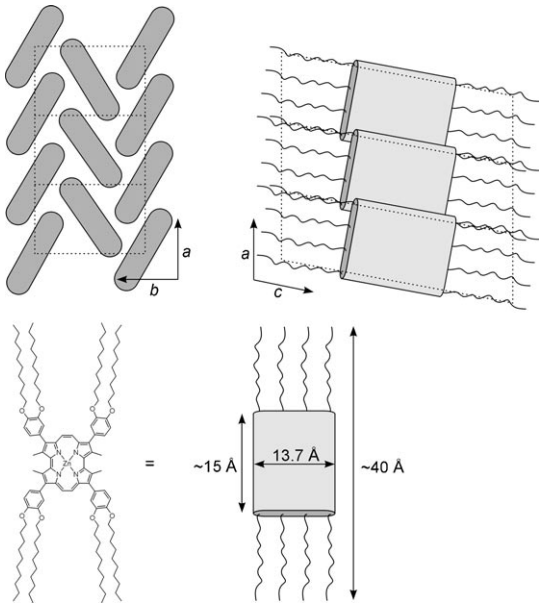

Figure 2. Proposed packing diagram for the L_{Col} phase of **1b**. The Figure is proportionally scaled, the thickness of the molecules being 3.6 Å. It should be noted that the aryl rings are not coplanar with the porphycene core.

original porphycene[43] (Figure 2). The packing can alternatively be viewed as a combination of tilted columnar stacks along *a*, with an antiparallel repeat of columns along *b*. If we assume that this repeat is generated by a 2_1 axis, the (010) reflections should be systematically absent, a conclusion that agrees with the experiment.

Phase behavior of porphyrins 2a,b: In analogy to what was seen in the case of the porphycene complex **1a**, the mixture of isomeric zinc porphyrins **2a** displayed no evidence of mesomorphic behavior. Rather, it exhibits a single crystalline phase which melts to produce an isotropic liquid at about 146 °C. Such behavior stands in contrast to the mesomorphism originally reported for zinc *meso*-tetra(*p*-alkoxyphenyl)porphyrins.[21] Subsequent studies revealed that these compounds were not in fact mesogenic,[52] and that the reported phases were actually crystalline. Moreover, the high enthalpies and microscopic textures provided for these previously reported compounds[21] are very similar to those observed for **1a** and **2a**, neither of which is mesogenic.

On the other hand, compound **2b** forms a liquid crystalline phase that is stable at room temperature and clears above 70 °C. The X-ray pattern of **2b**, recorded at 70 °C (Figure 3), is consistent with a centered columnar rectangular phase Col_r where the columns are packed in accord with an overall *c2mm* symmetry. The two intense and sharp small-angle reflections were indexed as the fundamental reflections (20) and (11) of a rectangular lattice. The indices of the remaining higher order reflections (Table 2) were deduced from the symmetry relationships of the *c2mm* plane group. These latter reflections are accompanied by two halos, one at 4.6 Å, corresponding to molten alkyl chains,

and another at 3.8 Å, ascribed to a stacking of the aromatic rings. The proposed model of the Col_r mesophase is shown in Figure 4. Molecules of **2b** are stacked into columns (1 molecule per columnar slice 3.8 Å thick), and their molecular planes are tilted with respect to the column axis. The columns then self-organize to produce the final two-dimensional centered rectangular lattice.

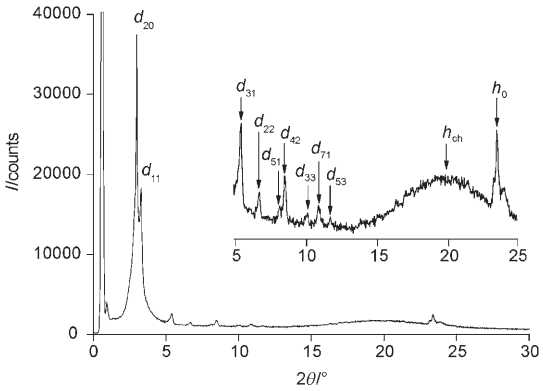

Figure 3. X-ray diffraction pattern of **2b** recorded at 70 °C.

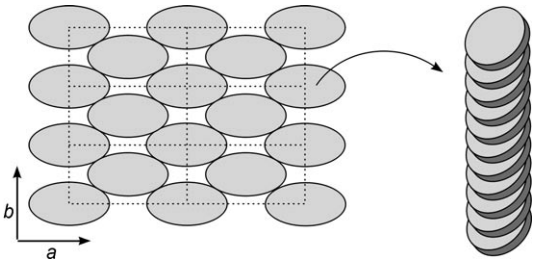

Figure 4. Proposed packing model for the Col_r *c2mm* mesophase of **2b**.

Formation and properties of the TCNQ adduct: Of the two porphycene complexes studied, only **1b** exhibits LC phases. However, the kinetic and thermodynamic stability of these latter phases is limited. We were, therefore, interested in exploring whether the mesomorphic behavior of **1b** could be enhanced via the addition of appropriately chosen small molecules. In one attempt made along these lines, the 1:1 adducts of **1a**,**b** and 4-(dimethylamino)pyridine (DMAP) were prepared. DMAP was chosen because it is known to form particularly stable complexes with zinc porphyrins.[53] In the case of the porphycenes **1a**,**b**, it was reasoned that the axially bound DMAP ligand would introduce an axial dipole that could improve the thermal stability of the liquid crystal phase. While an increase in the melting temperatures was observed, unfortunately, neither **1a**·DMAP nor **1b**·DMAP showed any mesomorphic properties.

Given this lack of success in terms of stabilizing a liquid crystalline phase, we decided to test the effect of combining **1b** with tetracyanoquinodimethane (TCNQ). TCNQ is one of several electron-deficient cyano compounds that form electron donor–acceptor (EDA) complexes with metalloporphyrins.[54–59] In fact, a number of EDA-stabilized liquid crystals are known,[60,61] including ferrimagnetically coupled columnar systems based on a Mn^{III} porphyrin.[62,63] The adduct **1b**·*n*TCNQ was thus prepared. This was done by taking a solution containing roughly equimolar amounts of **1b** and TCNQ and subjecting it to precipitation from MeOH/CH_2Cl_2. The properties of the resulting adduct are strongly dependent on workup conditions, which is probably a consequence of small variations in the overall complex stoichiometry.

Variable-temperature POM observations showed that **1b**·*n*TCNQ is crystalline from ambient temperature up to about 110 °C. Above this temperature, the material undergoes a phase transition, eventually yielding a homogeneous texture consisting of large cylindrical domains (Figure 5).

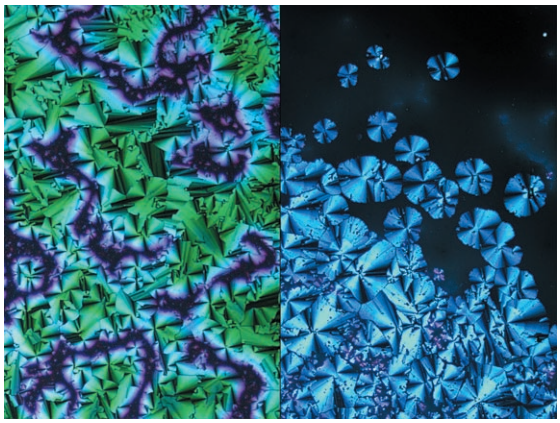

Figure 5. Polarizing optical microscopy textures of **1b**·*n*TCNQ obtained by heating the solid powder to 180 °C (left image) and by cooling the isotropic melt (right image).

The phase is fluid and retains its birefringence up to about 200 °C, at which point it clears into the isotropic liquid phase. The clearing process is largely irreversible, a finding that is considered due to phase separation (**1b**·*n*TCNQ cannot be generated by fusing its components). However, if the isotropic liquid is cooled immediately after clearing most of the mesophase is recovered. The resulting texture is identical with that obtained on heating. However, the pattern only forms locally and is not as uniformly distributed, showing a mixture of isotropic and birefringent zones.

The XRD pattern recorded for **1b**·*n*TCNQ at 140 °C is shown in Figure 6. It is characterized by the presence of three sharp small angle X-ray reflections, with reciprocal spacings in the ratio $1:\sqrt{3}:2$. These three features are most readily assigned as the (10), (11), and (20) reflections of a hexagonal lattice with a parameter $a = 28.9$ Å. The presence of two broad halos at 4.6 Å (h_{ch}) and at 8.15 Å (h) confirmed the fluid nature of the mesophase, the former signal corresponding to the molten chains in liquid-like order. An additional sharper signal was seen at 3.3 Å (h_0), corresponding to the stacking of consecutive aromatic molecules.

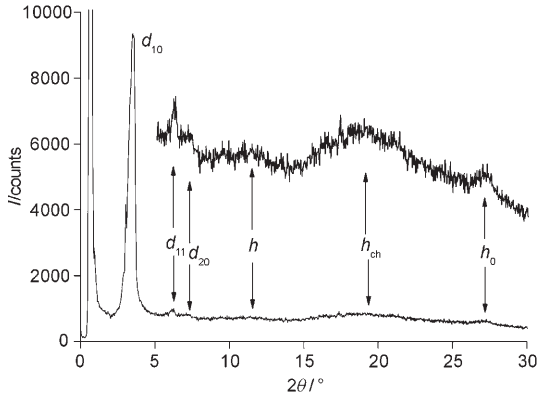

Figure 6. X-ray diffraction pattern obtained for **1b**·*n*TCNQ at 140 °C.

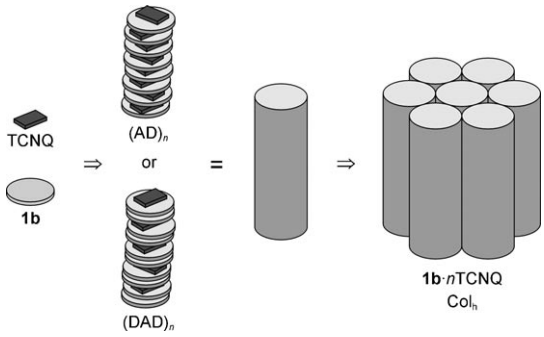

Figure 7. Proposed structural model for the mesophase produced by **1b**·*n*TCNQ.

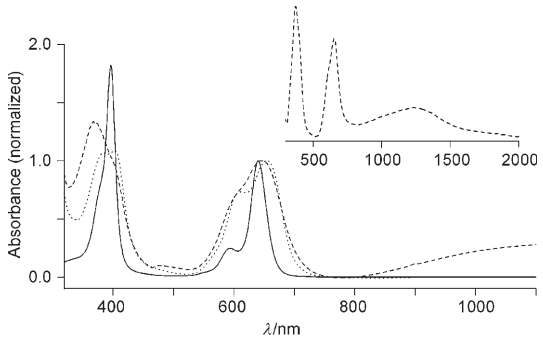

Figure 8. UV-vis-NIR electronic absorption spectra of **1b** (dilute CH_2Cl_2 solution, —— and thin film, •••••) and **1b**·*n*TCNQ (thin film, -----). Spectra were corrected for scattering and normalized to the intensity of the most intense Q band. The inset shows the entire spectrum of the **1b**·*n*TCNQ film.

Due to purification problems, attempts to determine the stoichiometry of **1b**·*n*TCNQ were not conclusive. Reported metalloporphyrin–TCNQ adducts characterized by X-ray crystallography have either 1:1 or 2:1 stoichiometry.[59] The 1:1 adducts consist of infinite alternating stacks of donor and acceptor molecules $(AD)_8$, whereas in the 2:1 systems the stacks are of the form $(DAD)_8$, with two metalloporphyrin molecules (D) acting to sandwich one TCNQ molecule (A). Using the column cross-section area determined by XRD and the estimated molecular volumes, it is possible to calculate the repeating periodicity along the column (*d*) for each stoichiometry (Table 2). The *d* values obtained for the 1:1 and 2:1 adducts are 5.46 and 10.42 Å, respectively. This corresponds to 2.73 and 3.47 Å per aromatic ring. Only the latter value matches the spacing between aromatic rings expected for stacked structures of this type. For instance, in the TCNQ–Cu(octaethylporphyrin) adducts, the π–π distances were in the range 3.29–3.31 Å.[59] Therefore, the stoichiometry of **1b**·*n*TCNQ can be tentatively assigned as close to 2:1. It is, however, possible that the actual stacking sequence may be partly disordered, that is, both 2:1 and 1:1 sequences are randomly interspersed, with only a short-range correlation length.

Figure 7 shows the proposed model for the **1b**·*n*TCNQ mesophase. The molecules of **1b** and TCNQ form columnar stacks as described above, which are further organized into a hexagonal array. As the column diameter (28.9 Å) is smaller than the diameter of an individual molecule of **1b** (with alkyl substituents fully extended), it is assumed that the chains are either partly coiled or that these substituents interdigitate between adjacent columns.

Manifestations of the EDA interaction between **1b** and TCNQ could be observed in the **1b**·*n*TCNQ adduct using UV/Vis-NIR spectroscopy (Figure 8). Comparison of the solid-state electronic spectra of **1b** and **1b**·*n*TCNQ revealed qualitative differences in the appearance of porphycene absorption bands (Soret and Q) indicating that the porphycene chromophore is affected by the presence of TCNQ. More importantly, an extremely broad and strongly red-shifted band (ca. 1200 nm, 8300 cm^{-1}) is observed for **1b**·*n*TCNQ. This band, which is absent in the spectrum of **1b**, corresponds to a charge transfer (CT) transition between **1b** and TCNQ.[55] When **1b**·*n*TCNQ is dissolved in CH_2Cl_2 the CT band is no longer observed, indicating that the EDA interaction is not operative in solution.

Additional insight into the structure of the **1b**·*n*TCNQ complex came from vibrational spectroscopy. The infrared spectrum of the adduct contains a series of bands at about 2200 cm^{-1}, which are absent in the spectrum of **1b**, and which correspond to the stretching vibrations of the CN bond (Figure 9). Variations in the frequency of the CN

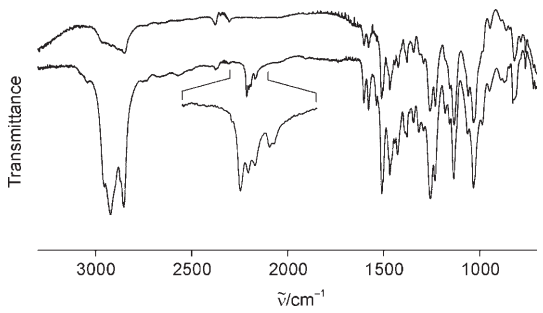

Figure 9. Vibrational spectra recorded for **1b** (upper trace) and **1b**·*n*TCNQ (lower trace). The region of CN stretching frequencies is expanded.

stretches are known to be correlated with the degree of charge transfer (Z) between the donor molecule (here **1b**) and TCNQ.[64] Of the five CN stretching bands observed for **1b**·*n*TCNQ, three correspond to Z values of 0.3, 0.5 and 0.8 (Table 3). The two remaining bands have significantly lower

Table 3. CN stretching frequencies and degrees of charge transfer for **1b**·*n*TCNQ and reference compounds.

Compound	$\approx\nu_{CN}$/cm^{-1}[a]	Z[b]
TCNQ[c]	2227	0.0
K^+[TCNQ]$^-$[c]	2183	1.0
1b·*n*TCNQ	2214	0.3
	2203	0.5
	2193	0.8
	2171	n/a
	2164	n/a

[a] CN stretching frequency (in cm^{-1}). [b] Degree of charge transfer calculated using the literature method.[64] [c] Literature data.[64]

frequencies, which would correspond to $Z > 1$. This apparent discrepancy can, however, be rationalized by assuming that some of the TCNQ molecules coordinate to the zinc ion of **1b** via a CN group.[57,58] To the extent this takes place, it is expected to result in an additional lowering of the stretching frequencies.

Conclusion

In this contribution we have shown for the first time that the use of porphyrins as the structural basis for mesogenic materials can be extended to include the quintessential porphyrin isomer porphycene. In the context of this work, we have found that the zinc porphycene **1b** is a particularly versatile system. It exhibits two structurally distinct mesophases, a discotic lamellar phase, Lam, and a lamello-columnar phase, L_{Col}, characterized by three-dimensional translational order. Such findings stand in marked contrast to what is seen in the case of the isomeric porphyrin system **2b**, which gives rise to a rectangular columnar phase. We have also found that porphycene **1b**, when combined with the electron acceptor TCNQ, forms a hexagonal columnar phase Col_h that exhibits improved thermal stability. Porphycene **1b** is, therefore, a novel adaptable system that can act as either a disc (in the Col_h phase) or a lath (in the Lam and L_{Col} phases). This diversity leads us to suggest that this and other porphyrin isomers may be further engineered to provide systems with very different packing geometries. Thus, in a broader sense, the findings reported herein provide support for the emerging notion that porphyrin analogues can be successfully exploited as structural motifs for the design of new mesogens and metallomesogens. This, in turn, could spawn new applications for discotic liquid crystals.

Experimental Section

General: Ethyl isocyanoacetate (Fluka), 1,8-diazabicyclo[5.4.0]undec-7-ene (DBU, Acros), di-*tert*-butyl dicarbonate (Acros), copper (99.7%, dendritic 3 μm, Aldrich) and 4-(dimethylamino)pyridine (DMAP, Aldrich) were used as received. Tetrahydrofuran, *N*,*N*-dimethylformamide (DMF), and toluene were dried by passing through activated alumina columns. Other solvents were reagent grade and used as received. Unless noted otherwise, TLC analyses were performed on analytical silica gel plates with a fluorescent indicator (Whatman) using 10% ethyl acetate in hexanes as the mobile phase.

Instrumentation and methods: Proton, ^{13}C, and two-dimensional NMR spectra were measured on Varian Unity Plus (300 MHz for ^{1}H), Varian Mercury (400 MHz), and Bruker Avance spectrometers (500 MHz). Unless noted otherwise, all spectra were recorded at room temperature. Gradient-selected ^{1}H,^{13}C correlation spectra were recorded with a resolution of 1024 to 2048 in the t_1 domain. Chemical shifts were referenced to residual solvent signals (7.24 ppm for C^1HCl_3 in $CDCl_3$, 77.0 ppm for $^{13}CDCl_3$). High-resolution chemical ionization (CI) mass spectra were obtained on a Waters (Micromass) Autospec mass spectrometer and the low-resolution electrospray ionization (ESI) spectrum was obtained on a Finnigan LCQ Classic mass spectrometer. Electronic spectra were obtained on a Cary 5000 UV/Vis-NIR spectrophotometer (courtesy of the Center for Nano- and Molecular Science and Technology at UT Austin). Elemental analyses were carried out at Midwest Microlab, Indianapolis, IN (USA). DSC data (30 to 220 °C, 10 deg per min) were collected using a Perkin Elmer DSC 7 calorimeter. DMAP-containing samples were crimped in airtight pans to reduce the loss of DMAP on heating. Optical microscopy observations were carried out using an Olympus BX41 polarizing microscope equipped with a hot stage (Instec Inc., model HCS402) and a 4 megapixel CCD camera.

XRD analysis: The XRD patterns were obtained with two different experimental set-ups. In all cases, a linear monochromatic $Cu_{K\alpha1}$ beam (λ = 1.5405 Å) was obtained using a sealed-tube generator (900 W) equipped with a bent quartz monochromator. In the first set-up, the transmission Guinier geometry was used, whereas a Debye–Scherrer-like geometry was used in the second experimental set-up. In all cases, the crude powder was filled in Lindemann capillaries of 1 mm diameter and 10 μm wall thickness. An initial set of diffraction patterns was recorded on an image plate; periodicities up to 80 Å can be measured, and the sample temperature controlled to within ±0.3 °C from 20 to 350 °C. The second set of diffraction patterns was recorded with a curved Inel CPS 120 counter gas-filled detector linked to a data acquisition computer; periodicities up to 60 Å can be measured, and the sample temperature controlled to within ±0.05 °C from 20 to 200 °C. In each case, exposure times were varied from 1 to 24 h.

Estimation of molecular volumes:[65–67] Molecular volumes V_{mol} were calculated using the formula:

$$V_{mol} = \frac{M}{\lambda \rho N_A}$$

where M is the molecular weight of the motif, N_A is the Avogadro number, ρ is the volume mass ($\approx$1 g cm^{-3}), and $\lambda(T)$ is a temperature correction coefficient at the temperature of experiment (T). It is defined as

$$\lambda = \frac{V_{CH_2}(T^0)}{V_{CH_2}(T)}$$

where

$$V_{CH_2}(T) = 26.5616 + 0.02023 \cdot T$$

is the volume of a methylene group (in Å^3) at a given temperature (in °C), and T^0 = 25 °C. (The temperature variation of molecular volume of the complex is expected to follow the trend determined experimentally for the methylene group).

Derivation of lattice parameters: The dimensions of the monoclinic cell of the **1b** LCol phase were obtained by numerical fitting to the experimental diffraction spacings using the formula

$$\frac{1}{d_{hkl}} = \sqrt{\frac{h^2}{a^2} + \frac{l^2}{c^2} + \frac{2hl\cos\beta}{ac}}{\sin^2\beta} + \frac{k^2}{b^2}$$

The intracolumnar repeating distance h is calculated directly from the estimated molecular volume according to

$$h = \frac{ZV}{S}$$

in which Z is the number of molecules (aggregation number) within the elementary fraction of the column (here Z is chosen equal to 1 as the molecule is disc-like), and S is the lattice area (columnar cross-section). For a hexagonal lattice

$$S = a^2 \frac{\sqrt{3}}{2}$$

where

$$a = \frac{2d_{10}}{\sqrt{3}}$$

is the lattice parameter obtained from the XRD analysis.

For the Lam phase: $A_{mol} = V_{mol}/d$, $A_{ch} = A_{mol}/N_{ch}$, where N_{ch} is the number of chains.

For the Col_r phase, the lattice parameters a and b are deduced from the following mathematical expression: $a = 2d_{20}$, and $1/d_{hk} = \sqrt{(h^2/a^2 + k^2/b^2)}$, where a, b are the parameters of the Col_r phase, S is the lattice area, S_{col} is the columnar cross-section ($S = a \times b$, $S_{col} = {}^1/_2 S$).

Syntheses of compounds **3**–**7** have been reported previously.[41]

General procedure for the formylation of α,α′-unsubstituted bipyrroles: In a 50 mL round-bottomed flask equipped with a stirring bar and a reflux condenser were placed an α-free bipyrrole (2 mmol), dry 1,2-dichloroethane (DCE, 15 mL) and absolute DMF (15 mL). The mixture was flushed with argon and cooled to 0 °C in an ice bath. Distilled $POCl_3$ (0.73 mL, 8 mmol) was added via a syringe within 30 minutes. The mixture was then heated to 60 °C in an oil bath and stirred for 1 hour. Subsequently the mixture was poured into aqueous sodium acetate (13 g per 100 mL of water) and heated to 85 °C for another hour. After cooling to room temperature, the mixture was extracted with DCE and then with dichloromethane. The combined organic extracts were dried using anhydrous sodium sulfate, and the solvent was removed on a rotary evaporator. The crude product was purified by flash column chromatography over silica gel (25% ethyl acetate/hexanes).

5,5′-Diformyl-3,3′-dimethyl-4,4′-bis(4-decyloxyphenyl)-2,2′-bipyrrole (8a): From **7a** (1.25 g, 2 mmol). Gray powder. Yield: 1.11 (82%). $R_f = 0.17$ (20% ethyl acetate/hexanes); ^{1}H NMR (300 MHz, $CDCl_3$): δ = 10.20 (b, 2H, N*H*), 9.41 (s, 2H, CHO), 7.32 (d, $^3J = 9.0$ Hz, 4H, phenyl 3,5-H), 6.98 (d, $^3J = 9.0$ Hz, 4H, phenyl 2,6-H), 4.00 (t, $^3J = 6.8$ Hz, 4H, α-decyl), 2.18 (s, 6H, pyrrole CH_3), 1.81 (m, 4H, β-decyl), 1.47 (m, 4H, γ-decyl), 1.38–1.20 (m, 24H, decyl CH_2), 0.87 ppm (t, $^3J = 6.8$ Hz, 6H, decyl CH_3); ^{13}C NMR (75 MHz, $CDCl_3$): δ = 179.82, 158.98, 137.30, 131.44, 129.87, 128.18, 124.20, 119.81, 114.52, 68.11, 31.90, 29.60, 29.57, 29.41, 29.32 (×2), 29.29, 26.07, 22.68, 14.12 ppm; HR-MS (CI+): *m*/*z*: calcd for $C_{44}H_{60}N_2O_4$: 680.4553; found: 680.4564 [M^+].

5,5′-Diformyl-3,3′-dimethyl-4,4′-bis(3,4-didecyloxyphenyl)-2,2′-bipyrrole (8b): From **7b** (0.94 mg, 1 mmol). Yield 0.75 g (76%). $R_f = 0.38$ (20% ethyl acetate/hexanes); ^{1}H NMR (300 MHz, $CDCl_3$): δ = 10.07 (br s, 2H, N*H*), 9.44 (s, 2H, CHO), 6.98–6.86 (m, 6H, *ortho* + *meta*), 4.04 (t, $^3J = 6.8$ Hz, 4H, decyl α-CH_2), 4.01 (t, $^3J = 6.8$ Hz, 4H, decyl α-CH_2), 2.19 (s, 6H, pyrrole CH_3), 1.90–1.76 (m, 8H, decyl β-CH_2), 1.5–1.40 (m, 8H, decyl γ-CH_2), 1.40–1.15 (m, 48H, decyl CH_2), 0.87 (t, $^3J = 6.8$ Hz, 6H, decyl CH_3), 0.85 ppm (t, $^3J = 6.8$ Hz, 6H, decyl CH_3); ^{13}C NMR (75 MHz, $CDCl_3$): δ = 179.87, 149.12, 148.87, 137.46, 129.86, 128.05, 124.64, 123.11, 119.78, 116.01, 113.49, 69.47, 69.24, 31.90, 29.66, 29.60, 29.57, 29.45, 29.35, 29.31, 26.07, 22.70, 14.10, 11.22 ppm; HR-MS (CI+): *m*/*z*: calcd for $C_{64}H_{101}N_2O_6$: 993.7660; found: 993.7656 [M+H$^+$].

General procedure for the synthesis of porphycenes via the McMurry coupling of diformylbipirroles: In a 250 mL three-necked round-bottomed flask equipped with a reflux condenser and a septum inlet were placed zinc powder (0.98 mg, 15.1 mmol) and copper(I) chloride (48 mg, 0.48 mmol). The apparatus was filled with argon and oxygen-free tetrahydrofuran (50 mL) was introduced through a cannula. Titanium tetrachloride (0.83 mL, 7.55 mmol) was added dropwise over 30 minutes using a syringe. The mixture was then heated under reflux for 3 h. Subsequently, a solution of diformylbipyrrole (0.30 mmol) in oxygen-free tetrahydrofuran (50 mL) was slowly added to the boiling mixture through a cannula. After completion of the addition (0.5–1 h), the septum was replaced with a glass stopper and the reaction mixture was kept under reflux for 12 h. After that time, the mixture was cooled down to room temperature and then to 0 °C using an ice bath. Aqueous ammonia (6%, 15 mL) was added dropwise over 1 h. The reaction mixture was then diluted with dichloromethane and filtered through a Celite plug, yielding a fluorescent yellow-orange filtrate that spontaneously changed color to green-blue upon contact with air. The plug was washed with more dichloromethane and the combined organic fractions were dried with anhydrous sodium sulfate. The solvents were removed under reduced pressure and the crude product was purified as described below.

3,6,13,16-Tetramethyl-2,7,12,17-tetrakis(4-decyloxyphenyl)porphycene (9a): From **8a** (500 mg, 0.73 mmol). The crude product was purified by column chromatography (200 mm × 35 mm, silica gel, 10% ethyl acetate/hexanes) and crystallized from dichloromethane/hexane to give a dark solid. Yield: 195 mg (41%). $R_f = 0.56$ (10% ethyl acetate/hexanes); ^{1}H NMR (300 MHz, $CDCl_3$): δ = 9.30 (s, 4H, *meso*-H), 7.83 (d, $^3J = 9.0$ Hz, 8H, phenyl 2,6-H), 7.24 (d, $^3J = 9.0$ Hz, 8H, phenyl 3,5-H), 4.16 (t, $^3J = 6.8$ Hz, 8H, decyl α-CH_2), 3.61 (s, 12H, pyrrole CH_3), 1.91 (m, 8H, decyl β-CH_2), 1.57 (m, 8H, decyl γ-CH_2), 1.48–1.22 (m, 48H, decyl CH_2), ≈1.24 (b, 2H, N*H*), 0.90 ppm (t, $^3J = 6.8$ Hz, 12H, decyl CH_3); ^{13}C NMR (75 MHz, $CDCl_3$): δ = 158.75, 143.66, 142.67, 137.51, 133.93, 131.57, 128.09, 114.40, 114.33, 113.49, 113.46, 68.24, 31.94, 29.66, 29.50, 29.43, 29.37 (×2), 26.18, 22.71, 17.46, 14.15 ppm, ; HR-MS (ESI+): *m*/*z*: calcd for $C_{88}H_{119}N_4O_4$: 1295.9231; found: 1295.9214 [M+H$^+$].

3,6,13,16-Tetramethyl-2,7,12,17-tetrakis(3,4-didecyloxyphenyl)porphycene (9b): From **8b** (428 mg, 0.431 mmol). The crude product was purified twice by flash column chromatography (250 mm × 35 mm, silica gel, 5% ethyl acetate/hexanes, then 2.5% ethyl acetate/hexanes). Finally, the product was triturated with hot methanol to give a viscous dark oil with blue luster. Yield: 137 mg (33%). $R_f = 0.84$ (10% ethyl acetate/hexanes); ^{1}H NMR (300 MHz, $CDCl_3$): δ = 9.33 (s, 4H, *meso*-H), 7.46 (d, $^4J = 1.7$ Hz, 4H, phenyl 2-H), 7.40 (dd, $^4J = 1.7$ Hz, $^3J = 8.1$ Hz, 4H, phenyl 6-H), 7.21 (d, $^3J = 8.1$ Hz, 4H, phenyl 5-H), 4.20 (t, $^3J = 6.8$ Hz, 8H, decyl α-CH_2), 4.14 (t, $^3J = 6.8$ Hz, 8H, decyl α-CH_2), 3.61 (s, 12H, pyrrole CH_3), 1.95 (m, 8H, decyl β-CH_2), 1.91 (m, 8H, decyl β-CH_2), 1.64–1.17 (m, 56H, decyl CH_2), 0.89 (t, $^3J = 6.8$ Hz, 12H, decyl CH_3), 0.83 ppm (t, $^3J = 6.8$ Hz, 12H, decyl CH_3), NH signal overlaps with the alkyl region; ^{13}C NMR (126 MHz, $CDCl_3$): δ = 148.88, 148.86, 143.94, 142.65, 137.57, 131.60, 128.64, 125.77, 118.56, 113.57, 69.56, 69.45, 31.96, 31.89, 29.72, 29.65, 29.64, 29.57, 29.54, 29.50, 29.48, 29.46, 29.40, 29.34, 26.19, 26.13, 22.72, 22.66, 17.49, 14.14, 14.08 ppm; MS (ESI+): *m*/*z*: calcd for $C_{128}H_{199}N_4O_8$: 1920.5; found: 1920.6 [M+H$^+$].

General procedure for the synthesis of β-aryl porphyrins: A suspension of lithium aluminium hydride (95 mg, 2.5 mmol) in dry tetrahydrofuran (35 mL) was placed in a 100 mL round-bottomed flask filled with argon and equipped with a stir bar and a septum inlet. A solution of the 2-ethoxycarbonyl ester derivative (**4a** or **4b**, 1 mmol) in dry tetrahydrofuran (15 mL) was quickly added with stirring. The progress of the reaction was monitored with thin layer chromatography. When the starting material was consumed ethyl acetate (10 mL) was added and the mixture was poured into aqueous ammonium chloride (50 mL). The mixture was extracted with dichloromethane, the combined organic extracts were dried with anhydrous potassium carbonate, and the solvent was removed under

reduced pressure. The resulting unstable carbinol (**10a** or **10b**) was dissolved in dry dichloromethane (90 mL) and placed under argon in a 250 mL round-bottomed flask equipped with a stir bar. Silica gel (500 mg) was then added and the reaction mixture was protected from light. After 20 h of stirring at room temperature 2,3-dichloro-5,6-dicyano-*p*-benzoquinone (DDQ, 170 mg, 0.75 mmol) was added and the solvent was removed on a rotary evaporator. The crude product (containing silica gel) was purified by flash column chromatography (200 mm × 25 mm, silica gel, dichloromethane).

Compound **11a** (mixture of isomers): From **5b** (385 mg, 1 mmol). Yield: 98 mg (30%, two steps). ^{1}H NMR (400 MHz, $CDCl_3$): δ = 10.04–10.23 (4H, *meso*-H), 8.09–7.95 (8H, phenyl 2,6-H), 7.37–7.19 (8H, phenyl 3,5-H), 4.21–4.08 (8H, decyl α-CH_2), 3.67–3.54 (12H, pyrrole CH_3), 1.99–1.87 (8H, decyl β-CH_2), 1.64–1.53 (8H, decyl γ-CH_2), 1.52–1.20 (48H, decyl CH_2), 0.92 (t, 12H, decyl CH_3), −3.46 ppm (b, 2H, N*H*); HR-MS (CI+): *m*/*z*: calcd for $C_{88}H_{119}N_4O_4$: 1295.9231; found: 1295.9214 [*M*+H$^+$].

Compound **11b** (mixture of isomers): From **5b** (200 mg, 0.37 mmol). Yield: 45 mg (26%, two steps). ^{1}H NMR (300 MHz, $CDCl_3$): δ = 10.15–10.29 (4H, *meso*-H), 7.77–7.29 (12H, phenyl 2,5,6-H), 4.31–4.00 (16H, decyl α-CH_2), 3.74–3.55 (12H, pyrrole Me), 2.06–1.88 (16H, decyl β-CH_2), 1.69–1.12 (112H, decyl CH_2), 0.89 (t, 12H, decyl CH_3), 0.81 (t, 12H, decyl CH_3), −3.44 ppm (b, 2H, N*H*); MS (CI+): *m*/*z*: calcd for $C_{128}H_{199}N_4O_8$: 1920.5; found: 1920 [*M*+H$^+$]; elemental analysis for $C_{128}H_{198}N_4O_8$: C 80.03, H 10.39, N 2.92; found: C 80.05, H 10.36, N 2.92.

General procedure for the Zn^{II} metallation of porphycenes and porphyrins: A free base porphycene or porphyrin (ca. 100 mg) and zinc(II) acetate dihydrate (fivefold molar excess) were dissolved in a mixture of chloroform (15 mL) and methanol (15 mL). The mixture was heated at reflux for 1 h and cooled to room temperature. The mixture was washed with water, the organic phase was dried with anhydrous sodium sulfate, and the solvents were removed under reduced pressure. Finally the product was recrystallized from dichloromethane/methanol. Yields were quantitative.

Compound **1a**: ^{1}H NMR (400 MHz, $CDCl_3$): δ = 9.48 (s, 4H, *meso*-H), 7.88 (d, ^3J = 9.0 Hz, 8H, phenyl 2,6-H), 7.27 (d, ^3J = 9.0 Hz, 8H, phenyl 3,5-H), 4.18 (t, ^3J = 6.8 Hz, 8H, decyl α-CH_2), 3.71 (s, 12H, pyrrole CH_3), 1.93 (m, 8H, decyl β-CH_2), 1.58 (m, 8H, decyl γ-CH_2), 1.48–1.25 (m, 48H, decyl CH_2), 0.90 ppm (t, ^3J = 6.8 Hz, 12H, decyl CH_3); ^{13}C NMR (126 MHz, $CDCl_3$): δ = 158.69, 146.93, 143.47, 141.64, 133.76, 131.64, 128.94, 114.34, 113.22, 68.26, 31.95, 29.68, 29.63, 29.52, 29.48, 29.38, 26.22, 22.72, 17.03, 14.14 ppm; UV/Vis (CH_2Cl_2, 298 K): λ_{max} (log ε, ε in $M^{-1}cm^{-1}$) = 396 (5.33), 595 (4.47), 642 nm (5.04); HR-MS (FAB): *m*/*z*: calcd for $C_{88}H_{116}N_4O_4Zn$: 1356.8288; found: 1356.8246 [*M*$^+$]; elemental analysis for $C_{88}H_{116}N_4O_4Zn$: C 77.76, H 8.60, N 4.12; found: C 77.52, H 8.41, N 4.16.

Compound **1b**: ^{1}H NMR (400 MHz, $CDCl_3$): δ = 9.59 (s, 4H, *meso*-H), 7.51 (d, ^4J = 1.7 Hz, 4H, phenyl 2-H), 7.48 (dd, ^4J = 1.7, ^3J = 8.1 Hz, 4H, phenyl 6-H), 7.25 (d, ^3J = 8.1 Hz, 4H, phenyl 5-H), 4.22 (t, ^3J = 6.8 Hz, 8H, decyl α-CH_2), 4.14 (t, ^3J = 6.8 Hz, 8H, decyl α-CH_2), 3.75 (s, 12H, pyrrole CH_3), 1.97 (m, 8H, decyl β-CH_2), 1.89 (m, 8H, decyl β-CH_2), 1.64–1.16 (m, 56H, decyl CH_2), 0.90 (t, ^3J = 6.8 Hz, 12H, decyl CH_3), 0.82 ppm (t, ^3J = 6.8 Hz, 12H, decyl CH_3); ^{13}C NMR (100 MHz, $CDCl_3$): δ = 148.73, 147.22, 143.45, 131.73, 129.47, 69.45, 59.48, 28.26, 31.97, 31.88, 29.74, 29.66 (×2), 29.57 (×2), 29.51 (×2), 29.45, 29.42, 29.34, 26.21, 26.12, 22.73, 22.65, 14.16, 14.08 ppm; UV/Vis (CH_2Cl_2, 298 K): λ_{max} (log ε, ε in $M^{-1}cm^{-1}$) = 271 (4.84), 396 (5.29), 594 (4.42), 640 nm (5.03); HR-MS (CI+): *m*/*z*: calcd for $C_{128}H_{197}N_4O_8Zn$: 1982.4423; found: 1982.4414 [*M*+H$^+$]; elemental analysis for $C_{128}H_{196}N_4O_8Zn$: C 77.48, H 9.96, N 2.82; found: C 77.66, H 10.01, N 2.86.

Compound **2a**: ^{1}H NMR (400 MHz, $CDCl_3$): δ = 9.12–10.06 (4H, *meso*-H), 8.08–7.91 (8H, phenyl 2,6-H), 7.42–7.24 (8H, phenyl 3,5-H), 4.29–4.16 (8H, decyl α-CH_2), 3.56–3.19 (12H, pyrrole CH_3), 2.05–1.92 (8H, decyl β-CH_2), 1.69–1.57 (8H, decyl γ-CH_2), 1.52–1.20 (48H, decyl CH_2), 0.95–0.87 ppm (t, 12H, decyl CH_3); UV/Vis (CH_2Cl_2, 298 K): λ_{max} (log ε, ε in $M^{-1}cm^{-1}$) = 411 (5.59), 537 (4.40), 575 nm (4.58); HR-MS (CI+): *m*/*z*: calcd for $C_{88}H_{116}N_4O_4Zn$: 1356.8288; found: 1356.8275 [*M*$^+$]; elemental analysis for $C_{88}H_{116}N_4O_4Zn$: C 77.76, H 8.60, N 4.12; found: C 77.52, H 8.62, N 4.07.

Compound **2b**: ^{1}H NMR (500 MHz, $CDCl_3$, data for isomer I only): δ = 10.20 (s, 4H, *meso*-H), 7.72 (d, ^4J = 2.0 Hz, 4H, phenyl 2-H), 7.67 (dd, ^4J = 2.0 Hz, ^3J = 8.2 Hz, 4H, phenyl 6-H), 7.35 (d, ^3J = 8.2 Hz, 4H, phenyl 5-H), 4.27 (t, ^3J = 6.8 Hz, 8H, decyl α-CH_2), 4.23 (t, ^3J = 6.8 Hz, 8H, decyl α-CH_2), 3.59 (s, 12H, pyrrole CH_3), 2.01 (m, 8H, decyl β-CH_2), 1.96 (m, 8H, decyl β-CH_2), 1.69–1.14 (m, 56H, decyl CH_2), 0.90 (t, ^3J = 6.8 Hz, 12H, decyl CH_3), 0.81 ppm (t, ^3J = 6.8 Hz, 12H, decyl CH_3); ^{13}C NMR (126 MHz, $CDCl_3$, data for isomer I only): δ = 149.39, 148.99, 148.77, 148.09, 142.45, 137.34, 129.42, 125.03, 118.44, 114.15, 100.88, 69.82, 69.75, 32.22, 32.12, 30.00, 29.93, 29.91, 29.86, 29.85, 29.82, 29.76, 29.74, 29.67, 29.57, 26.51, 26.43, 22.98, 22.89, 14.38, 14.30, 12.75 ppm; UV/Vis (CH_2Cl_2, 298 K): λ_{max} (log ε, ε in $M^{-1}cm^{-1}$) = 412 (5.47), 538 (4.33), 575 nm (4.51); elemental analysis for $C_{128}H_{196}N_4O_8Zn$: C 77.48, H 9.96, N 2.82; found: C 77.86, H 10.38, N 2.44.

Preparation of DMAP complexes: The zinc(II) porphycene (ca. 20 μmol) and 4-(*N*,*N*-dimethylamino)pyridine (6 mg, ca. 5 equiv) were dissolved in a mixture of dichloromethane (5 mL) and methanol (5 mL). Dichloromethane was then slowly removed on a rotary evaporator until the entire product precipitated from the solution. The precipitate was then decanted and dried under vacuum.

Compound **1a**·DMAP: ^{1}H NMR (400 MHz, $CDCl_3$): δ = 9.36 (s, 4H, *meso*-H), 7.88 (d, ^3J = 7.8 Hz, 8H, phenyl 2,6-H), 7.25 (d, ^3J = 7.8 Hz, 8H, phenyl 3,5-H), 4.64 (d, ^3J = 6.8 Hz, 2H, pyridine *meta*-H), 4.17 (t, ^3J = 6.3 Hz, 8H, decyl α-CH_2), 3.62 (s, 12H, pyrrole CH_3), 2.52 (br d, ^3J = 6.8 Hz, 2H, pyridine *ortho*-H), 2.11 (b, 6H, NMe_2), 1.93 (m, 8H, decyl β-CH_2), 1.62–1.22 (m, 56H, decyl CH_2), 0.90 ppm (t, ^3J = 6.8 Hz, 12H, decyl CH_3).

Compound **1b**·DMAP: ^{1}H NMR (300 MHz, $CDCl_3$): δ = 9.42 (s, 4H, *meso*-H), 7.53 (b, 4H, phenyl 2-H), 7.46 (≈d, phenyl 6-H), 7.23 (d, 4H, phenyl 5-H), 4.79 (b, 2H, pyridine *meta*-H), 4.22 (t, ^3J = 6.8 Hz, 8H, decyl α-CH_2), 4.17 (t, ^3J = 6.8 Hz, 8H, decyl α-CH_2), 3.96 (b, 2H, pyridine *ortho*-H), 3.64 (s, 12H, pyrrole CH_3), 2.23 (b, 6H, NMe_2), 1.96 (m, 8H, decyl β-CH_2), 1.91 (m, 8H, decyl β-CH_2), 1.64–1.16 (m, 56H, decyl CH_2), 0.90 (t, ^3J = 6.8 Hz, 12H, decyl CH_3), 0.82 ppm (t, ^3J = 6.8 Hz, 12H, decyl CH_3).

Preparation of 1b·*n*TCNQ: A solution of **1b** (40 mg, ca. 20 mmol) in dichloromethane (10 mL) was combined with tetracyanoquinodimethane (4.8 mg, 1.2 equiv) dissolved in methanol (20 mL). Dichloromethane was slowly removed on a rotary evaporator (at normal pressure) thereby allowing the porphycene material to precipitate completely. The mother liquor was carefully removed with a syringe and the resulting precipitate was dried under vacuum.

Acknowledgements

This work was supported by the US National Science Foundation (grant no. CHE-0515670 to J.L.S.), CNRS, and the University Louis Pasteur-Strasbourg, France (financial support to B.D.). Thanks are given to Phillip-Morris USA for supplying the polarizing microscope and the Texas Materials Institute for allowing use of the differential scanning calorimeter. M.S. thanks the University of Wrocław for providing access to an NMR spectrometer. We also thank Vladimir Roznyatovskiy for his help in obtaining microanalytical data for compound **11b**.

[1] S. Chandrasekhar, B. K. Sadashiva, K. A. Suresh, *Pramana* **1977**, *9*, 471–480.
[2] E. Dalcanale in *Comprehensive Supramolecular Chemistry, Vol. 10* (Eds.: J. L. Atwood, J. E. D. Davies, D. D. MacNicol, F. Vögtle, D. N. Reinhoudt), Pergamon, Oxford **1996**, p. pp. 583–635.
[3] N. Boden, B. Movaghar in *Handbook of Liquid Crystals, Vol. 2B* (Eds.: D. Demus, J. Goodby, G. W. Gray, H.-W. Spiess, V. Vill), Wiley-VCH, Weinheim, **1998**, pp. 798.

[4] R. J. Bushby, O. R. Lozman, *Curr. Opin. Colloid Interface Sci.* **2002**, *7*, 343–354.
[5] J. Simon, P. Bassoul, *Design of Molecular Materials: Supramolecular Engineering*, Wiley-VCH, Weinheim, **2001**.
[6] J. Nelson, *Science* **2001**, *293*, 1059–1060.
[7] V. Percec, M. Glodde, T. K. Bera, Y. Miura, I. Shiyanovskaya, K. D. Singer, V. S. K. Balagurusamy, P. A. Heiney, I. Schnell, A. Rapp, H.-W. Spiess, S. D. Hudson, H. Duan, *Nature* **2002**, *419*, 384–387.
[8] L. Schmidt-Mende, A. Fechtenkötter, K. Müllen, E. Moons, R. H. Friend, J. D. MacKenzie, *Science* **2001**, *293*, 1119–1122.
[9] J. Y. Kim, A. J. Bard, *Chem. Phys. Lett.* **2004**, *383*, 11–15.
[10] M. A. Fox, J. V. Grant, D. Melamed, T. Torimoto, C. Liu, A. J. Bard, *Chem. Mater.* **1998**, *10*, 1771–1776.
[11] B. A. Gregg, M. A. Fox, A. J. Bard, *J. Phys. Chem.* **1990**, *94*, 1586–1598.
[12] C. Liu, H. Pan, M. A. Fox, A. J. Bard, *Science* **1993**, *261*, 897–899.
[13] S. Kumar, *Liq.Cryst.* **2005**, *32*, 1089–1113.
[14] M. D. Watson, A. Fechtenkötter, K. Müllen, *Chem. Rev.* **2001**, *101*, 1267–1300.
[15] H. Eichhorn, *J. Porphyrins Phthalocyanines* **2000**, *4*, 88–102.
[16] C. A. Hunter, J. K. M. Sanders, *J. Am. Chem. Soc.* **1990**, *112*, 5525–5534.
[17] B. Donnio, D. Guillon, D. W. Bruce, R. Deschenaux, in *Comprehensive Coordination Chemistry II: From Biology to Nanotechnology, Vol. 7* (Eds.: J. A. McCleverty, T. J. Meyer), Elsevier, Oxford **2003**, pp. 357–627.
[18] J. W. Goodby, P. S. Robinson, B.-K. Teo, P. E. Cladis, *Mol. Cryst. Liq. Cryst.* **1980**, *56*, 303–309.
[19] B. A. Gregg, M. A. Fox, A. J. Bard, *J. Chem. Soc. Chem. Commun.* **1987**, 1134–1135.
[20] B. A. Gregg, M. A. Fox, A. J. Bard, *J. Am. Chem. Soc.* **1989**, *111*, 3024–3029.
[21] S. Kugimiya, M. Takemura, *Tetrahedron Lett.* **1990**, *31*, 3157–3160.
[22] Y. Shimizu, M. Miya, A. Nagata, K. Ohta, I. Yamamoto, S. Kusubayashi, *Liq. Cryst.* **1993**, *14*, 795–805.
[23] A. Nagata, Y. Shimizu, H. Nagamoto, M. Miya, *Inorg. Chim. Acta* **1995**, *238*, 169–171.
[24] L. R. Milgrom, G. Yahioglu, D. W. Bruce, S. Morrone, F. Z. Henari, W. J. Blau, *Adv. Mater.* **1997**, *9*, 313–315.
[25] K. Ohta, N. Yamaguchi, I. Yamamoto, *J. Mater. Chem.* **1998**, *8*, 2637–2650.
[26] B. R. Patel, K. S. Suslick, *J. Am. Chem. Soc.* **1998**, *120*, 11802–11803.
[27] K. Ohta, N. Ando, I. Yamamoto, *Liq. Cryst.* **1999**, *26*, 663–668.
[28] V. Paganuzzi, P. Guatteri, P. Riccardi, T. Sacchelli, J. Barbera, M. Costa, E. Dalcanale, *Eur. J. Org. Chem.* **1999**, 1527–1539.
[29] M. Castella, F. López-Calahorra, D. Velasco, H. Finkelmann, *Chem. Commun.* **2002**, 2348–2349.
[30] T. Sugino, J. Santiago, Y. Shimizu, B. Heinrich, D. Guillon, *Liq. Cryst.* **2004**, *31*, 101–108.
[31] J. L. Sessler, A. Gebauer, E. Vogel, in *The Porphyrin Handbook, Vol. 2* (Eds.: K. M. Kadish, K. M. Smith, R. Guilard), Academic Press, San Diego, CA **2000**, pp. 1–54.
[32] J. L. Sessler, D. Seidel, *Angew.Chem.* **2003**, *115*, 5292–5333; *Angew. Chem. Int. Ed.* **2003**, *42*, 5134–5175.
[33] R. Paolesse, in *The Porphyrin Handbook, Vol. 2* (Eds.: K. M. Kadish, K. M. Smith, R. Guilard), Academic Press, San Diego, CA **2000**, pp. 201–232.
[34] J. L. Sessler, A. Gebauer, S. J. Weghorn in *The Porphyrin Handbook, Vol. 2* (Eds.: K. M. Kadish, K. M. Smith, R. Guilard), Academic Press, San Diego, CA **2000**, pp. 55–124.
[35] L. Latos-Grażyński in *The Porphyrin Handbook, Vol. 2* (Eds.: K. M. Kadish, K. M. Smith, R. Guilard), Academic Press, New York **2000**, pp. 361–416.
[36] T. D. Lash, in *The Porphyrin Handbook, Vol. 2* (Eds.: K. M. Kadish, K. M. Smith, R. Guilard), Academic Press, San Diego, CA **2000**, pp. 125–199.
[37] D. Seidel, V. Lynch, J. L. Sessler, *Angew.Chem.* **2002**, *114*, 1480–1483; *Angew. Chem. Int. Ed.* **2002**, *41*, 1422–1424.
[38] P. J. Chmielewski, L. Latos-Grażyński, K. Rachlewicz, *Chem. Eur. J.* **1995**, *1*, 68–73.
[39] A. Jasat, D. Dolphin, *Chem. Rev.* **1997**, *97*, 2267–2340.
[40] J. L. Sessler, W. B. Callaway, S. P. Dudek, R. W. Date, V. Lynch, D. W. Bruce, *Chem. Commun.* **2003**, 2422–2423.
[41] M. Stępień, B. Donnio, J. L. Sessler, *Angew.Chem.* **2007**, *119*, 1453–1457; *Angew. Chem. Int. Ed.* **2007**, *46*, 1431–1435.
[42] J. L. Sessler, W. B. Callaway, S. P. Dudek, R. W. Date, D. W. Bruce, *Inorg. Chem.* **2004**, *43*, 6650–6653.
[43] E. Vogel, M. Köcher, H. Schmickler, J. Lex, *Angew.Chem.* **1986**, *98*, 262–264; *Angew. Chem. Int. Ed. Engl.* **1986**, *25*, 257–259.
[44] D. H. R. Barton, J. Kervagoret, S. Z. Zard, *Tetrahedron* **1990**, *46*, 7587–7598.
[45] E. Vogel, P. Koch, X.-L. Hou, J. Lex, M. Lausmann, M. Kisters, M. A. Aukauloo, P. Richard, R. Guilard, *Angew. Chem.* **1993**, *105*, 1670–1673; *Angew. Chem. Int. Ed. Engl.* **1993**, *32*, 1600–1604.
[46] N. Ono, K. Maruyama, *Chem. Lett.* **1989**, 1237–1240.
[47] N. Ono, H. Kawamura, M. Bougauchi, K. Maruyama, *Tetrahedron* **1990**, *46*, 7483–7496.
[48] B. Alameddine, O. F. Aebischer, W. Amrein, B. Donnio, R. Deschenaux, D. Guillon, C. Savary, D. Scanu, O. Scheidegger, T. A. Jenny, *Chem. Mater.* **2005**, *17*, 4798–4807.
[49] C. W. Struijk, A. B. Sieval, J. E. J. Dakhorst, M. van Dijk, P. Kimkes, R. B. M. Koehorst, H. Donker, T. J. Schaafsma, S. J. Picken, A. M. van de Craats, J. M. Warman, H. Zuilhof, E. J. R. Sudholter, *J. Am. Chem. Soc.* **2000**, *122*, 11057–11066.
[50] G. Zucchi, B. Donnio, Y. H. Geerts, *Chem. Mater.* **2005**, *17*, 4273–4277.
[51] A. Gavezzotti, *Acta Crystallogr. Sect. B* **1990**, *46*, 275–283.
[52] Y. Shimizu, M. Miya, A. Nagata, K. Ohta, A. Matsumura, I. Yamamoto, S. Kusabayashi, *Chem. Lett.* **1991**, 25.
[53] K. M. Kadish, L. R. Shiue, R. K. Rhodes, L. A. Bottomley, *Inorg. Chem.* **1981**, *20*, 1274–1277.
[54] D. A. Summerville, T. W. Cape, E. D. Johnson, F. Basolo, *Inorg. Chem.* **1978**, *17*, 3297–3300.
[55] L. J. Pace, A. Ulman, J. A. Ibers, *Inorg. Chem.* **1982**, *21*, 199–207.
[56] D. M. Eichhorn, S. Yang, W. Jarrell, T. F. Baumann, L. S. Beall, A. J. P. White, D. J. Williams, A. G. M. Barrett, B. M. Hoffman, *J. Chem. Soc. Chem. Commun.* **1995**, 1703–1704.
[57] K. Sugiura, K. Ushiroda, M. T. Johnson, J. S. Miller, Y. Sakata, *J. Mater. Chem.* **2000**, *10*, 2507–2514.
[58] W. Hibbs, A. M. Arif, M. Botoshansky, M. Kaftory, J. S. Miller, *Inorg. Chem.* **2003**, *42*, 2311–2322.
[59] M. M. Olmstead, A. de Bettencourt-Dias, H.-M. Lee, D. Pham, A. L. Balch, *Dalton Trans.* **2003**, 3227–3232.
[60] F. D. Saeva, G. A. Reynolds, L. Kaszczuk, *J. Am. Chem. Soc.* **1982**, *104*, 3524–3525.
[61] K. Praefcke, J. D. Holbrey, *J. Inclusion Phenom. Mol. Recognit. Chem.* **1996**, *24*, 19–41.
[62] K. Griesar, M. A. Athanassopoulou, E. A. Soto Bustamante, Z. Tomkowicz, A. J. Zaleski, W. Haase, *Adv. Mater.* **1997**, *9*, 45–48.
[63] J. P. Hill, T. Sugino, Y. Shimizu, *Mol. Cryst. Liq. Cryst.* **1999**, *332*, 119–125.
[64] J. S. Chappell, A. N. Bloch, W. A. Bryden, M. Maxfield, T. O. Poehler, D. O. Cowan, *J. Am. Chem. Soc.* **1981**, *103*, 2442–2443.
[65] F. Morale, R. W. Date, D. Guillon, D. W. Bruce, R. L. Finn, C. Wilson, A. J. Blake, N. Schröder, B. Donnio, *Chem. Eur. J.* **2003**, *9*, 2484–2501.
[66] B. Donnio, B. Heinrich, H. Allouchi, J. Kain, S. Diele, D. Guillon, D. W. Bruce, *J. Am. Chem. Soc.* **2004**, *126*, 15258–15268.
[67] D. Guillon, *Struct. Bonding (Berlin)* **1999**, *95*, 41–82.

Received: January 24, 2007
Published online: June 14, 2007

